MECHANICAL MODEL OF *CERASUS HUMILIS* ESTABLISHED BY UNIAXIAL COMPRESSION PHYSICAL TEST AND VIRTUAL SIMULATION
/
基于单轴压缩物理试验和虚拟仿真的钙果力学模型构建

Shilei KANG[1,2], Jiaxuan LU[1], Huhu YANG[1], Yanxi GUO[1], Junlin HE*[1,2]
[1]College of Agricultural Engineering, Shanxi Agricultural University, Taigu 030801, China;
[2]Dryland Farm Machinery Key Technology and Equipment Key Laboratory of Shanxi Province, Taigu 030801, China
Tel: +86-0354-6288400; E-mail: hejunlin26@126.com
Corresponding author: Junlin HE
DOI:https://doi.org/10.35633/inmateh-69-50

Keywords: *Cerasus humilis*, *uniaxial compression, elastic–plastic model, optimization*

ABSTRACT
The mechanical parameters of Cerasus humilis are the basic data for subsequent studies on fruit deformation, damage, and movement characteristics during harvesting and transportation, but these parameters are rarely reported. Relevant mechanical parameters of whole fruit compression are calculated by comparing physical tests and virtual simulations. The orthogonal rotating combined experimental design was used to arrange the simulation tests, with the elastic modulus (E), yield limit (E_y), and tangent modulus (E_t) as the influence factors and compression force as the result. Response surface optimization was employed to find the closest test point to the force–deformation curve of the physical test. The parameters of the pulp test point are as follows: E = 0.923 MPa, E_y = 0.0897 MPa, and E_t = 0.478 MPa. Results show that the step on the force–deformation curve was not the beginning of the pulp yield, which was substantially earlier than the strain rate at the simulation step. The region of increased stress in the pulp first appeared at the junction with the core due to stress concentration. Combining virtual and physical tests to solve the mechanical parameters of fruits is more suitable than testing the standard pulp sample.

摘要
钙果的力学参数是后续研究果实在采收和运输过程中变形、损伤和运动特性的基础数据，但这些参数的报道很少。通过物理试验和虚拟仿真的结合，计算了全果压缩的相关力学参数。采用正交旋转组合试验设计，以弹性模量(E)、屈服极限(E_y)和切线模量(E_t)为影响因素，压缩力为结果，设计了虚拟试验方案。采用响应面优化方法，寻找最接近物理试验力–变形曲线的试验点。果肉测点参数为:E = 0.923 MPa, E_y = 0.0897 MPa, E_t = 0.478 MPa。结果表明:果肉屈服的起始点并非力–变形曲线上的阶跃点，而是明显早于阶跃点的应变率。由于应力集中，果肉中应力增加的区域首先出现在与果核的交界处。将虚拟试验和物理试验相结合来求解水果的力学参数，比测试标准果肉样品更合适。

INTRODUCTION
Cerasus humilis, a type of tiny fruit, has been selected from wild plums by fruit experts in China in recent decades. In the process of brush harvesting, fruits, branches, and comb teeth contact each other, and these contact behaviours will induce fruit crushing and damage. Moreover, this fruit will also be squeezed until damaged during fruit packaging, transportation, storage, and other links. Therefore, extrusion is an important damage cause, and studying the mechanical behaviour of *Cerasus humilis* under extrusion is necessary.

In the research on the mechanical properties of extrusion contact of fruits, a testing method similar to that of metal materials was used by *Shirvani (2014*), *Alamar (2008), and Celik (2021)* to examine fruits with cut standard shape samples. However, this method ignores that the fruit comprises materials of different properties and disregards the influence of the complex structure of the fruit on its stress and deformation, which is inappropriate for fruit with continuous production links. The uniaxial plate compression test of whole fruit is most suitable to simulate the stress phenomenon during fruit production.

Tian (2017) stated that although physical tests can obtain the relationship between force and deformation of fruit, the distribution of stress inside the fruit is unavailable. By contrast, computer simulation techniques can perform the aforementioned task.

[1] *Shilei KANG,As Lec.PhD. Eng; Jiaxuan LU,M.S. Eng; Huhu YANG,M.S. Eng; Yanxi GUO,M.S. Eng; Junlin HE,Prof.Ph.D.Eng.*

Dintwa (2008) and *Rashvand (2022)* stated that the finite element method was commonly used to calculate the internal stress distribution of complex structures. *Liu (2022)* and *Wang (2006)* indicated that the method can analyse the effects of various fruit parts. The distribution of stress is of considerable importance to the study of fruit damage under the action of external load. At present, the force–deformation curve obtained from the compression of the whole fruit with a rigid flat cannot be converted into the real stress–strain relationship of fruit materials. Therefore, this paper will use the method of combining physical tests and simulations to study the mechanical behaviour of the whole fruit under compression to explore the distribution of stress and strain inside the fruit and the physical properties of related materials.

MATERIALS AND METHODS

Physical test of uniaxial compression

In this experiment, *Cerasus humilis* "Nongda No.4", which met the harvest requirement, was collected in Juxin Modern Agriculture Demonstration Park in Shanxi Province in the morning of September 3, 2021, in a sunny day. The entire branch was cut and brought back to the laboratory, the incision was immersed in water to keep the branches active, and all the tests were completed within 4 h. During the experiment, fruits were individually picked from the branches, the stalks were removed, the surfaces were wiped, and the bad fruits with abnormal development and pests were discarded. Fruits with approximate symmetry along the calyx–stalk axis were selected as test samples.

A CMT6104 microcomputer control electronic universal testing machine, which can automatically collect the compression deformation and its corresponding force in the test process, was used. The force sensor with a range of 500 N was chosen, and a circular flat plate indenter with a diameter of 100 mm was selected. The falling speed of the indenter is 5 mm/min, and the data sampling frequency is 15 Hz.

Before the compression test, an electronic vernier calliper was utilized to measure the 3D size of the sample. Measurement results revealed that the fruit was slightly small in the longitudinal (Z) direction and slightly large in the transverse (XOY) direction perpendicular to it, demonstrating a nearly circular cross-section (as shown in Fig. 1a). Many simulation times are needed in this study. The axial compression model can be simplified into a plane one, which can markedly reduce the calculation scale compared with transverse compression. Therefore, only axial compression data are used for research. Fig. 1b shows the physical compression test. At least 20 valid sample data are obtained by compression until the fruit breaks.

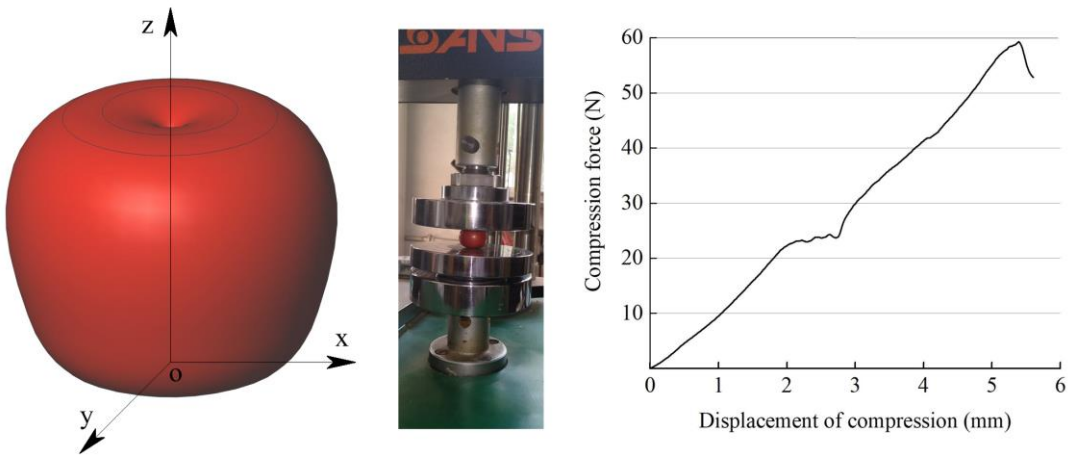

(a) (b) (c)

Fig. 1 - 3D model, physical test, and typical force–deformation curve

Fig.1c shows a typical force–deformation curve from the uniaxial compression test. All the sample curves showed a temporary step, which was not accidental; this step was not caused simply by the pulp yield but the macroscopic manifestation of partial separation of pulp and core or the partial rupture and collapse of pulp. According to previous compression tests on standard-shaped pulp samples of *Shirvani (2014)*, the deformation rate of pulp yield is often considerably smaller than that of the step in this paper, and the appearance of step is not the beginning of yield. For the whole fruit comprising multiple materials, the step on the force–deformation curve does not correspond to the yield phenomenon on the stress–strain curve obtained by the test of the standard shape sample made of pulp.

The fruit structure has been destroyed when the internal pulp damage has occurred at the step of the force–deformation curve. In the work on the whole fruit, its deformation rate generally does not reach this step. The deformation rate corresponding to this step is approximately 10% in the force–deformation curves of all samples. Therefore, only the part of the curve before the step is conducted in the simulation test.

Virtual test of uniaxial compression

Virtual geometric model

The typical force–deformation curve of uniaxial compression is taken as the comparison standard. Sample data near the average value were selected to realize representativeness. The fruit of the same size as the sample was measured in 3D and then cut in half along the meridian with a sharp knife and photographed. The shape of this fruit was traced with a pen after the section was attached to the paper (dimensions: longitudinal 16.0 mm, transverse average 19.98 mm). Fig. 2 shows the longitudinal section of *Cerasus humilis*, which comprises three parts, namely core, pulp, and peel. The core is small and ellipsoidal, with long and short semi-axes of approximately 5 and 3 mm, respectively. The peel is thin and dense, and the pulp is carefully scraped off with a knife and the thickness of the peel is about 0.1 mm measured with an electronic vernier calliper. The images were fitted with a spline curve in CAD software to fit the shape and position relationship of each part. These images were then scaled to the measured dimensions to make a 3D compression model (shown in the cross-section in Fig. 2), and the cross-section of the axisymmetric model was extracted as the simulation analysis object.

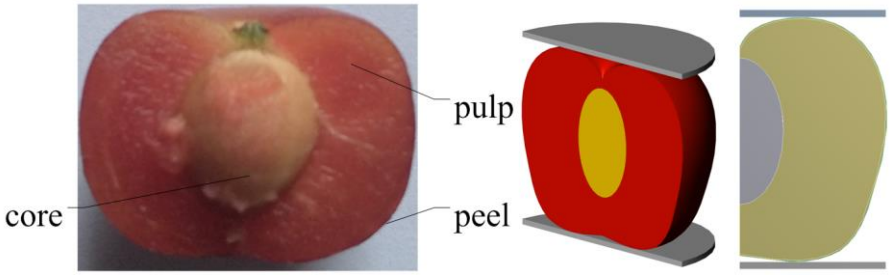

Fig. 2 - Anatomical structure and geometric model

Mechanical properties

The relevant physical parameters of each structure of the model should be generally obtained before the simulation test. The upper and lower plates are stainless steel indenters in physical tests and can be set as rigid bodies in the simulation. The core of the fruit is a wooden structure with a hard texture, and its stiffness is several orders of magnitude larger than that of the pulp. The core can also be set as a rigid body in the simulation.

Most fruit materials demonstrate an elastic behaviour under a small strain. An increase in strain shows elastic–plastic deformation, and a continuous strain increment shows full-plastic deformation. At the macro level, the fruit demonstrates irreversible deformation until rupture. *Kim (2008)* regarded fruits as completely elastic materials and applied Hertz theory to explain mechanical phenomena, which is true under remarkably small strains. However, the strain in this study becomes seriously asynchronous and demonstrates the stress concentration phenomenon due to the existence of a hardcore. Thus, even if the whole fruit has only a small strain, its local strain will be several times that of the whole strain. Alamar *(2008)* stated that the strain was only approximately 5% when the modulus of elasticity was calculated in accordance with the stress–strain curve obtained from the standard cuboid apple pulp sample test. *Cerasus humilis* and “Golden Delicious” apple have a similar texture; thus, the elastic limit strain of *Cerasus humilis* should also be similar. Under the overall strain of 10% in this study, the local stress concentration of pulp facilitated the entrance of part of pulp stress in the plastic stage. Therefore, the completely elastic model was inappropriate. Pulp was not used as a viscoelastic material but as an elastoplastic material because viscoelasticity is unsuitable to express the permanent damage caused by fruits exceeding the yield limit, and the elastoplastic model is simple. *Celik (2017)* stated that fruit materials were assumed to be isotropic elastoplastic materials and are often characterized by bilinear hardening models. Consider the fruit as a multibody system, where each part was regarded as a uniform material by *Li (2013)*.

The pulp comprises cells with sufficient moisture content, which is determined to be more than 90%. Previous researchers used moulds to cut standard samples when testing the modulus of elasticity of large fruits, such as an apple with similar materials to calcium pulp. However, the fruit size in this study is too small to make standard shape samples.

More importantly, a considerable amount of water is lost during compression, and its boundary conditions are completely different from those in the whole fruit tests. As for the modulus of elasticity of fruit peel, *Juxia (2015)* and *Hetzroni (2011)* separated the peel and pulp of apples and tomatoes to make approximately rectangular samples. This method has several disadvantages; fruit peel and pulp are often closely combined, and pulp residue will emerge in the samples. Moreover, spherical fruit peel cannot be expanded into a plane theoretically, and a serious uneven force exists in the cross-section of the sample during the tensile test. Therefore, the value range of the elastic modulus of pulp and peel is estimated in accordance with the order of magnitude of similar fruits. This range is adjusted and optimized in the simulation test, until the force–deformation curve obtained in the simulation and physical tests is consistent.

The fruit was treated as a single completely elastic material, and the calculated apparent elastic modulus of the whole fruit of "Nongda No.4" *Cerasus humilis* by Hertz contact theory is 0.66 MPa according to *Zhibin (2016)*. A total of 0.5–1.5 MPa was taken as the optimal range of the elastic modulus of pulp because of the wide elastic modulus range of biomaterials with different maturities. The yield limit of pulp may also have a certain influence on the mechanical behaviour in compression. The yield limit is usually proportional to the elastic modulus, which is set as 10% of the elastic modulus in a previous study. The tangent modulus is the slope between yield and strength limits on the stress–strain curve of the material. According to previous studies on standard apple samples, it is approximately one-third of elastic modulus *(Zhe, 2016*) and is preset to 0.15–0.5 MPa.

Cerasus humilis and *"Golden Delicious" apple* are all thin-peel fruits. The peel mainly plays the role of preventing water loss, oxidation, and the invasion of outside bacteria. The bearing capacity of fruit peel is limited, and the mechanical parameters of fruit pulp dominate the force–deformation relationship during fruit compression. *Juxia (2015)* stated that the elastic modulus of peel was one order of magnitude higher than that of pulp. The peel possibly remains in the elastic stage under the deformation rate of fruit in this study. Therefore, only the elastic modulus of the peel is considered.

When measuring the Poisson's ratio of pulp, 20 standard-shaped fruits were selected and numbered as samples and fresh weight was measured. The fruits were then naturally air-dried, the dry core was obtained, the powder of pulp and the peel was also acquired. The core and the powder were weighed, and the moisture content of the pulp and the peel mixture was calculated. Separating pulp and peel under dry and wet conditions is difficult, and the calculated moisture content is also the sum of the two. The average moisture content of 20 samples is 93%. The formula (1) was used to calculate the Poisson's ratio by *Ashtiani (2019)*.

$$\mu = 0.1 + 0.4 * M \quad (1)$$

where: M is the average moisture content, [%]; μ is the Poisson's ratio, which is calculated to be 0.47, and it can be approximated as the Poisson's ratio of pulp, because the mass of the peel in the powder is remarkably small.

Finite element model, load, boundary conditions, and meshing

In the uniaxial compression fruit model, the upper and lower plates are round and their connecting line is coaxial with the symmetry axis of the fruit. The fruit surface is tangent to the upper and lower plates. The model is simplified to a 2D axisymmetric plane model because of its axisymmetric characteristics. The contact between pulp and core (Nongda No.4 is adherent stone) and between peel and pulp should be bonded contact. The upper and lower plates comprise stainless steel; therefore, the contact type with the fruit is frictional contact. Except for axial movement, frictionless constraints were applied to the symmetry axes of the upper and lower plates and the fruit to limit their degrees of freedom. The lower plate imposed fixed constraints to limit all degrees of freedom. *Jackson (2005)* stated two load application methods to the upper plate: applying force and displacement loads. The displacement load has a faster convergence rate than the force load. Therefore, 1.6 mm displacement is applied on the upper plate (corresponding to 10% strain) and the compression speed is the same as the physical test (5 mm/min), which is in line with the standard of *ASAE (2022).*

The separate structures of core, pulp, and peel are combined into a whole before mesh division. Therefore, common nodes can be generated on the contact surface during mesh in the later stage, which is conducive to improving the calculation stability. In the meshing, the contact region of each structure is refined to simulate the curve deformation accurately. The mesh size away from the contact area gradually increases with a growth rate of 1.1 times and is dominated by quadrilateral meshes. The specific mesh size is gradually refined until the pulp stress obtained by calculation stabilizes. The corresponding force is equal to the compression reaction force in the simulation when the displacement load is applied to the upper plate.

Simplification of the geometric model

In the simulation, an accurate virtual model is always needed to represent the physical model. Simultaneously, the model should be as simple as possible to reduce the calculation scale. Many assumptions were made in the modelling process, and the material properties of various parts and the connections between them in the model may be different from the real situation. However, the virtual model is considered reasonable as long as the deformation of the simulation model under the same external load is consistent with the real physical test results and the distribution of internal stress conforms to the mechanical law.

Whether the peel and pulp can be considered as a whole is a problem to be discussed when deliberating the distribution and change in stress inside the fruit under a 10% compression rate. Stripping the peel is difficult; therefore, measuring its physical parameters is also difficult. Moreover, only one reference standard is used to verify the virtual model, that is, the force–deformation curve obtained from physical tests. Therefore, if the peel model parameters were added, then the unknown quantity of the virtual model would be excessive and difficult to establish.

A simulation test was then conducted to calculate the stress distribution and change process of pulp in the compression process to determine the retention of fruit peel in the virtual model. The peel is assumed to be a part of the pulp; therefore, only two types of material are left in the fruit model: the core and the pulp. The core is regarded as a rigid body, and the material parameters that must be adjusted and optimized belong to the pulp. The pulp model parameters include elastic modulus E, Poisson's ratio μ, yield strength E_y, and tangent modulus E_t. The elastic modulus is estimated to be approximately 0.9 MPa according to the previous analysis, the yield limit is 10% of the elastic modulus, the Poisson's ratio is 0.47, and the tangent modulus is 0.3 MPa. The meshing, boundary conditions, and load of the model are consistent with those mentioned above. After constant adjustment of the calculation, the distribution and variation trend of stress and strain in the fruit can be considered reasonable until the force–deformation curve obtained from the virtual test is close to the corresponding physical test result.

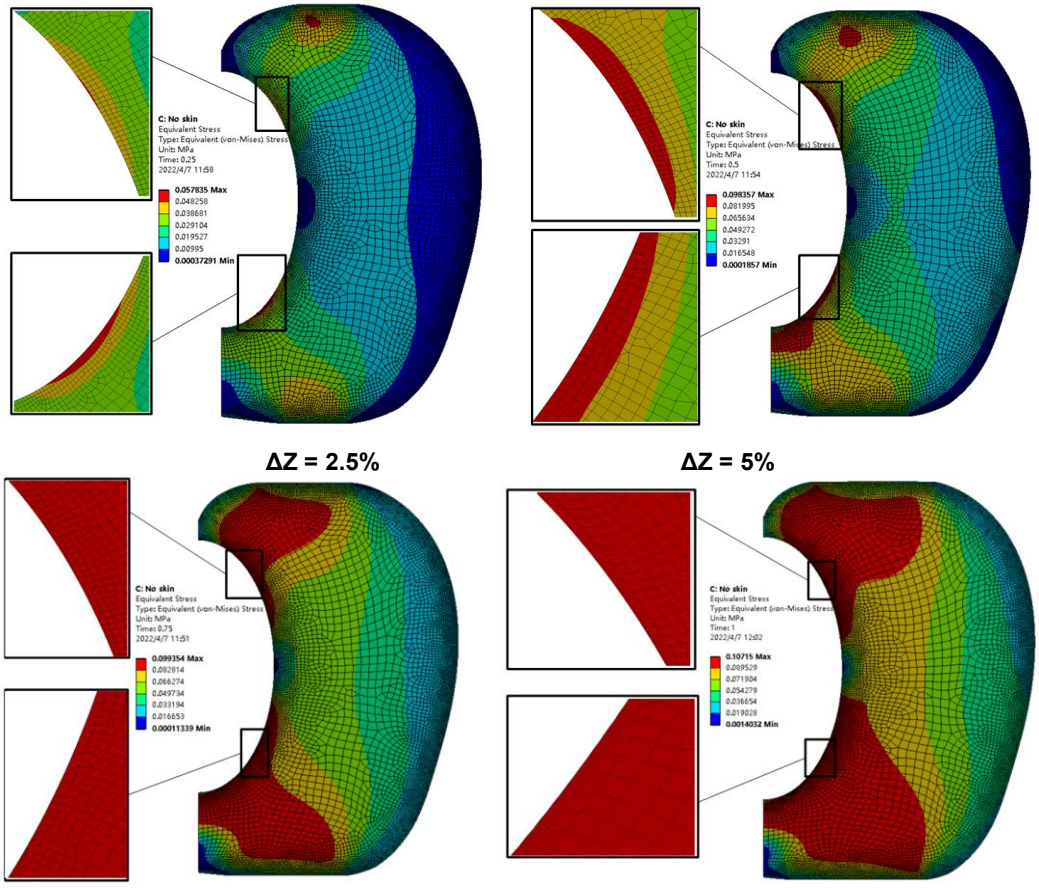

Fig. 3 - Distribution and variation of equivalent stress of pulp

Zulkifli (2020) stated that fruits comprise materials with different properties, and the inhomogeneity of materials and their connections seriously affect the stress distribution of fruit. The peel and core of different fruits have varying effects on the stress distribution of pulp.

Fig. 3 shows the equivalent stress distribution and variation of pulp during virtual compression. The stress increase in pulp starts from two different regions: one is at the junction of the core and the other is at a certain distance under the peel of the part in contact with the flat plate. The equivalent stress gradually increases to the yield limit with the compression ratio, and then the yield region continues to expand. The maximum stress occurs at the junction with the core, followed by a certain depth under the peel of the contact part. This phenomenon is due to the stiffness difference of several orders of magnitude between the pulp and the core, and the strain of the pulp and the core is seriously asynchronous when the fruit is subjected to external compression, resulting in serious asynchronicity at the interface between the pulp and the core and inducing shear stress. However, the increase in stress near the contact region with the upper and lower parts and the flat plate is relatively lagging. The yield region of pulp does not extend to the peel even when the overall compression rate reaches 10%. However, at this time, the mesh of part of the pulp at the junction with the core was considerably distorted, indicating that the shearing stress of this part of the pulp had reached a remarkably serious degree, and some pulp was almost destroyed. This phenomenon did not occur farther away from the pit. This finding is inconsistent with the observed phenomenon in the compression simulation of the apple by *Fenyvesi (2013)*. The apple is a no stone fruit while *Cerasus humilis* is a stone fruit; thus, the difference in the internal structure of the two results in different stress distributions.

This experiment reveals that the stress distribution in the fruit is seriously affected by the wooden core. The region exceeding the yield limit did not extend to the fruit surface until the compression rate in this study according to the stress distribution and its development. Therefore, within the range of compression rate in this study, taking the peel as a part of the pulp without separate modelling is reasonable when investigating the fruit deformation behaviour.

Virtual experiment design

The pulp parameters to be determined in this study include elastic modulus E, yield limit E_y, and tangent modulus E_t, which are respectively represented by codes X_1, X_2, and X_3, and the compression reaction force Y is used as the test index. The rotating centre composite design method was utilized to arrange the test to determine the relationship between the influence factors and the test index. As the number of factors is 3, the number of second-level comprehensive tests is 8, and the number of asterisk tests is 6. The number of zero-level tests is 1 because it is a simulation test. The length of the asterisk arm is calculated from the number of zero- and two-level tests. The level codes and parameter values of each factor are shown in Table 1, and the coded quadratic regression orthogonal rotation combination test sites are shown in Table 2.

Table 1

Factors and levels

Level code	Factor		
	X_1 [MPa]	X_2 [MPa]	X_3 [MPa]
r (1.215)	1.5	0.15	0.5
1	1.3	0.13	0.429
0	1	0.1	0.325
−1	0.7	0.07	0.221
−r (1.215)	0.5	0.05	0.15

Table 2

CCD design scheme and experimental results

Serial number	X_1	X_2	X_3	X_1X_2	X_1X_3	X_2X_3	X_1^2	X_2^2	X_3^2	Y
1	1	1	1	1	1	1	1	1	1	23.6
2	1	1	−1	1	−1	−1	1	1	1	22.9
3	1	−1	1	−1	1	−1	1	1	1	19
4	1	−1	−1	−1	−1	1	1	1	1	17.2
5	−1	1	1	−1	−1	1	1	1	1	14
6	−1	1	−1	−1	1	−1	1	1	1	13.9
7	−1	−1	1	1	−1	−1	1	1	1	13.3
8	−1	−1	−1	1	1	1	1	1	1	12.7
9	r	0	0	0	0	0	r^2	0	0	22.7
10	−r	0	0	0	0	0	r^2	0	0	9.96
11	0	r	0	0	0	0	0	r^2	0	19.4
12	0	-r	0	0	0	0	0	r^2	0	14.2
13	0	0	r	0	0	0	0	0	r^2	18.7
14	0	0	-r	0	0	0	0	0	r^2	17.6
15	0	0	0	0	0	0	0	0	0	18.2

RESULTS

Statistical analysis of experiment results

The experiment results of quasistatic compression simulation were obtained, as shown in Table 2. The analysis of variance (ANOVA) was applied to the experiment results by Design-Expert 8.0.6. All factors and interactions were included in the first ANOVA. The analysis revealed that the F values of interaction terms X_1X_3, X_2X_3, and quadratic term X_3^2 were less than 1, indicating that the influence of these items on the results could be ignored. Therefore, these items were incorporated into the residual term and ANOVA was conducted again, as shown in Table 3.

According to ANOVA, modulus of elasticity E (X_1) had the highest significant level of compression force, sequentially followed by yield limit E_y (X_2) and modulus of tangent E_t (X_3). Simultaneously, the interaction X_1X_2 and quadratic terms X_1^2 and X_2^2 had a certain impact on the compression force.

The post-ANOVA information also provided a prediction of coefficient estimates and their standard errors for a predictive regression model. The quadratic regression between modulus of elasticity (X_1), yield limit (X_2), modulus of tangent(X_3), and compression force(Y) is computed as follows:

$$Y = -1.88 + 16.22X_1 + 39.86\ X_2 + 3.56\ X_3 + 117.84\ X_1\ X_2 - 7.78\ X_1^2 - 531.7\ X_2^2 \quad (2)$$

ANOVA was conducted for the above regression model and a significance test was performed. The results are shown in Table 3. The coefficient of determination of the model is $R^2 = 0.9955$ and F is substantially higher than $F_{0.01}(6,8)$, indicating that the multiple regression model is extremely significant and the regression equation is effective.

Table 3

Analysis of variance

Source	SS	DF	MS	F-value	P-value	Sig
X_1	188.45	1	188.45	1400.64	<0.0001	***
X_2	32.12	1	32.12	238.76	<0.0001	***
X_3	1.87	1	1.87	13.88	0.0058	**
X_1 X_2	8.82	1	8.82	65.56	<0.0001	***
X_1^2	4.74	1	4.74	35.21	0.0003	**
X_2^2	2.21	1	2.21	16.46	0.0036	**
Model	236.50	6	39.42	292.96	<0.0001	***
Residual	1.08	8	0.13			

*Notes: SS is the sum of squares, DF is degrees of freedom, MS is mean square, F-value is statistics value, Sig is significance, ***means P < 0.001,** means P < 0.01, $F_{0.01}(1,8) = 11.26$, $F_{0.01}(6,8) = 6.37$.*

Influence of a single factor on the compression reaction force

Fig. 4 was drawn on the basis of simulation test data. Fig. 4a reveals the relationship between the compression force and the gradient of a single factor (the modulus of elasticity). The curve showed an increasing trend with the elastic modulus of pulp, which was consistent with previous cognition. When the elastic modulus increased from 0.5 MPa to 1.5 MPa, the compression force of the whole fruit increased from 9.96 N to 22.75 N and the compression force was highly sensitive to the elastic modulus. ANOVA results also reveal that elastic modulus has a significant influence on compression reaction force. With the increase in elastic modulus, the gradient of compression force decreases from 24% to less than 3% at 1/8 intervals in the range of 0.5–1.5 MPa.

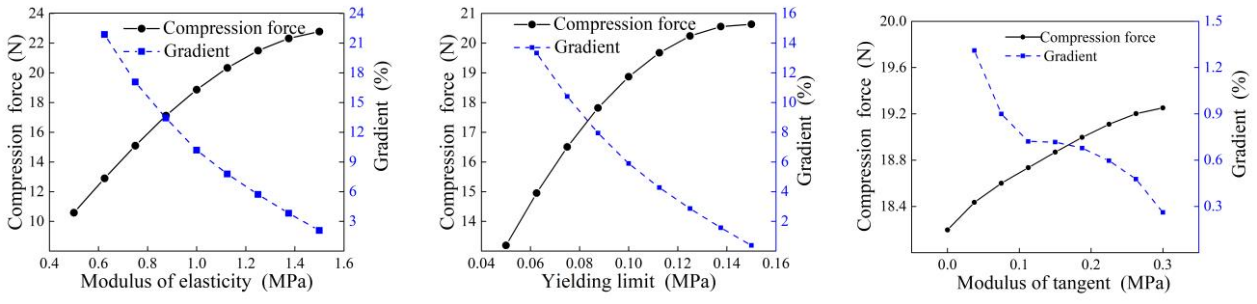

(a) (b) (c)

Fig. 4 - Effects of physical parameters of pulp on fruit compression force

Fig. 4b reveals the relationship between the compression force and the gradient of a single factor (the yield limit). The figure shows that the compression force increases with the yield limit. When the yield limit increases from 0.05 MPa to 0.15 MPa, the compression force rises from 14.2 N to 19.4 N and its sensitivity to the yield limit is also substantially high. ANOVA results also indicate that the yield limit has a remarkably significant influence on the compression force. The increment in compression force gradually decreases with the increase in yield limit. The gradient of compression force decreases from 9.9% to 1.1% at 1/8 intervals under range of 0.05–0.15 MPa.

Fig. 4c reveals the relationship between the compression force and the gradient of a single factor (the tangent modulus). The figure shows that although the compression force also demonstrates an increasing trend with the tangent modulus, its change rate is within 1% in all test levels. The compression force only increases by 5% when the tangent modulus rises from 0.15 MPa to 0.5 MPa. The compression force is insensitive to the change in tangent modulus. ANOVA results also demonstrate that the significance level of tangent modulus is lower than the two other factors.

Influence of interaction on compression force

Fig. 5 shows the response surface and contour to the reaction force of compression as a function of modulus of elasticity (X_1) and yield limit (X_2). The influence factors of X_1 and X_2 were significant at 0.01 probability level by the F test of ANOVA, and their interaction was also significant at 0.01 probability level. The overall effect of the two main influence factors on the reaction force of compression was observed in the response surface. The compression reaction tends to increase with the rise in elastic modulus and yield limit. The interaction terms X_1X_3 and X_2X_3 related to X_3 in the first ANOVA have been excluded. Therefore, analysing the response surfaces of the two interactions is no longer necessary.

The quadratic terms X_1^2 and X_2^2 were also significant at the 0.01 probability level in the ANOVA of the model.

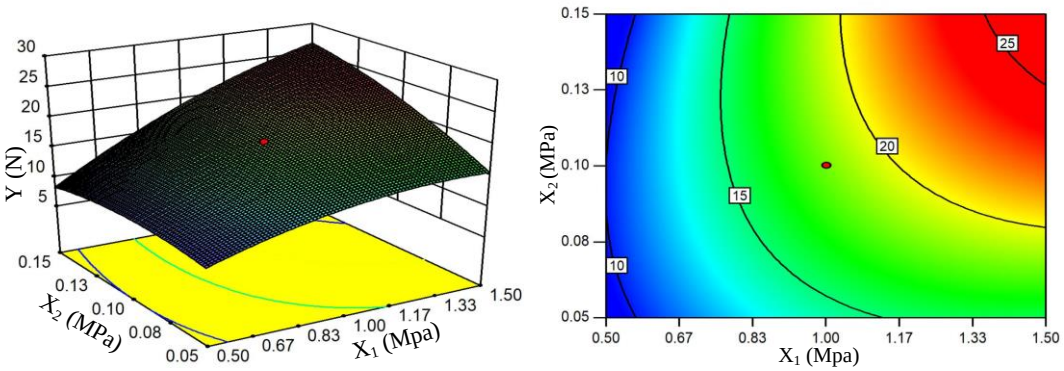

Fig. 5 - Response surface and contour of elastic modulus (X_1) and yielding limit (X_2)

Optimization

The optimization design method is originally used in structural or technological design to find the optimal scheme according to the predetermined objective under certain constraints. The material properties of pulp are inherent and cannot be designed. However, pulp materials are often uneven and anisotropic, and their inherent properties remarkably vary with different positions. A set of simplified equivalent parameters is needed to represent the pulp to study the mechanical behaviour of fruits at the macro scale. Thus, the obtained parameters are not necessarily the real properties of the pulp, but their combination can approximate the physical model. Moreover, measuring the real properties of the pulp of small berries with high moisture content is difficult. Therefore, the specific value of this parameter combination must be determined or designed. Response surface optimization (RSM) can use appropriate strategies to find the optimal parameters for pulp model construction.

Taking the compression force of 17.1 N under 10% strain in the physical test curve as the optimization object, three candidate points were given by the RSM algorithm, as shown in Table 4. The force–deformation curves corresponding to the three points were obtained and plotted on the same coordinate plane as the physical test curve, as shown in Fig. 6. The cubic regression equations of the physical test and three candidate point curves in the figure (intercept was set as 0) are shown in Table 4. The table reveals that the regression equation of candidate Point 1 is closest to the physical test; therefore, its parameter value can be used as the material parameter of the pulp sample studied in this test.

Table 4

Physical test and candidate points

	E (MPa)	E_y (MPa)	E_t (MPa)	Y (N)	Equation of regression
Physical test				17.1	$y = 0.318x^3 + 1.038x^2 + 8.266x$ ($R^2 = 0.997$)
Candidate 1	0.923	0.0897	0.478	17.2	$y = -1.657x^3 + 5.49x^2 + 6.156x$ ($R^2 = 1$)
Candidate 2	1.1	0.0666	0.39	17.0	$y = -2.229x^3 + 5.147x^2 + 8.015x$ ($R^2 = 0.998$)
Candidate 3	0.955	0.0889	0.339	17.1	$y = -2.006x^3 + 5.893x^2 + 6.352x$ ($R^2 = 0.999$)

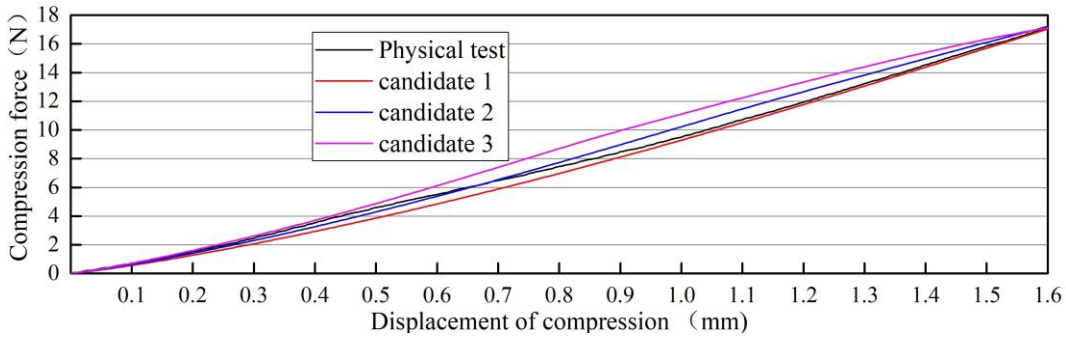

Fig. 6 - Force–deformation curves of physical test and three candidate points

CONCLUSIONS

(1) In the uniaxial compression of the whole "Nongda No.4" *Cerasus Humilis*, the step on the force–deformation curve was not the beginning of pulp yield but the partial tear at the pulp–core junction and the collapse of pulp at a certain distance under the peel of the contact point with the flat plate.

(2) When looking for the combination of parameters in the virtual pulp model, the regression equation between the compression force and each parameter was obtained by the central combination rotation orthogonal test method and the model was remarkably significant.

(3) The parameter value combination, which can represent the physical model of the pulp, can be obtained through the combination of physical and simulation tests and certain optimization strategies. The virtual model constituted by this parameter combination can replace the physical model and the stress distribution and variation inside the fruit, which cannot be observed by the physical test, can also be realized.

ACKNOWLEDGEMENT

This research, titled "Mechanical model of *Cerasus humilis* established by uniaxial compression physical test and virtual simulation", was funded by project: "Science and Technology Innovation Fund of Shanxi Agricultural University (Grant No. 2017017)", and was also supported by "Shanxi Basic Research Program (Grant No. 202203021221174)".

REFERENCES

[1] Alamar M. C., Vanstreels E., Oey M. L., Moltó E., & Nicolai B. M., (2008). Micromechanical behaviour of apple tissue in tensile and compression tests: Storage conditions and cultivar effect. *Journal of Food Engineering*, 86(3), 324-333;

[2] ASAE., (2022), Compression test of food materials of convex shape, ASAE S368.4 DEC2000(R2022);

[3] Ashtiani S.M., Sadrnia H., Mohammadinezhad H., Aghkhani M.H., Khojastehpour M., & Abbaspour-Fard M.H., (2019), Fem-based simulation of the mechanical behaviour of grapefruit under compressive loading, *Scientia Horticulturae,* 245, 39-46;

[4] Celik K. H. (2017), Determination of bruise susceptibility of pears (Ankara variety) to impact load by means of fem-based explicit dynamics simulation. *Postharvest Biology & Technology,* 128:83-97;

[5] Celik H. K., Ustun H., Erkan M., Rennie A. E., & Akinci I., (2021), Effects of bruising of 'Pink Lady' apple under impact loading in drop test on firmness, colour and gas exchange of fruit during long term storage, *Postharvest Biology and Technology*, 179, 111561;

[6] Dintwa E., Zeebroeck M.V., Ramon H., Tijskens E., (2008), Finite element analysis of the dynamic collision of apple fruit. *Postharvest Biology & Technology*, 49(2):260-276;
[7] Fenyvesi L., Fenyvesi D., & Csatár A., (2013), Stress analysis in fruits. *Advances in Mechanical Engineering,* 5, 874673;
[8] Hetzroni A., Vana A., & Mizrach A., (2011), Biomechanical characteristics of tomato fruit peels. *Postharvest Biology & Technology,* 59(1):80-84;
[9] Jackson R. L., & Green I., (2005), A Finite Element Study of Elasto-Plastic Hemispherical Contact Against a Rigid Flat. *Journal of Tribology,* 127(2):343-354;
[10] Juxia W., Qingliang C., Hongbo, L., & Yaping L., (2015), Experimental research on mechanical properties of apple peels. *Journal of Engineering and Technological Sciences,* 47(6):688-705;
[11] Kim G.W., Do G.S., Bae Y., & Sagara Y., (2008), Analysis of mechanical properties of whole apple using finite element method based on three-dimensional real geometry. *Food Science & Technology Research,* 14(4):329-336;
[12] Li Z., Yang H., Li P., Liu J., Wang J., Xu Y., (2013), Fruit biomechanics based on anatomy: a review. *International Agrophysics,* 27(1):97-106;
[13] Liu X., Cao Z., Yang L., Chen H., & Zhang Y., (2022), Research on Damage Properties of Apples Based on Static Compression Combined with the Finite Element Method. *Foods*, 11(13), 1851;
[14] Rashvand M., Altieri G., Genovese F., Li Z., & Di Renzo G. C., (2022), Numerical simulation as a tool for predicting mechanical damage in fresh fruit, *Postharvest Biology and Technology*, 187, 111875;
[15] Shirvani M., Ghanbarian D., & Ghasemi-Varnamkhasti M., (2014), Measurement and evaluation of the apparent modulus of elasticity of apple based on Hooke's, Hertz's and Boussinesq's theories, *Measurement,* 54:133-139;
[16] Tian K., Cheng S., Li X., Huang J., & Zhang B., (2017), Mechanical properties and compression damage simulation by finite element for kiwifruit, *International Agricultural Engineering Journal,* 26(4):191-201;
[17] Wang C.X., Pritchard J., & Thomas C. R., (2006), Investigation of the mechanics of single tomato fruit cells. *Journal of Texture Studies,* 37(5):597-606;
[18] Zhe Feng., (2016), *Measurement of contact pressure of apple under different loads and bruising predication using finite element analysis （苹果不同受载时接触应力测量分析及损伤预测）*, Master Thesis, Shihezi University, China;
[19] Zhibin Sun., (2016), *Experimental Research of Branches Feeding Device of Cerasus humilis (钙果枝条喂入装置的试验研究),* Master Thesis, Shanxi Agricultural University, China;
[20] Zulkifli N., Hashim N., Harith H. H., & Shukery M. F. M., (2020). Finite element modelling for fruit stress analysis-A review. *Trends in Food Science & Technology*, 97, 29-37;